# Dynamic mechanical behaviour of highly oriented poly(oxymethylene) produced by microwave heat-drawing

**K. Nakagawa and T. Konaka**
*NTT Ibaraki Electrical Communication Laboratories, Nippon Telegraph and Telephone Corporation, Tokai, Ibaraki, 319-11, Japan*
*(Received 1 April 1985; revised 17 September 1985)*

Dynamic mechanical measurements on highly oriented poly(oxymethylene) produced by microwave heat-drawing have been undertaken at four frequencies (3.5, 11, 35 and 110 Hz) over the temperature range from −150°C to the melting point. The dynamic modulus at 110 Hz reached a value of 85 GPa at −150°C for the most highly-oriented sample (draw ratio, 41). The $\alpha$ and $\gamma$ absorptions are clearly discernible, even at the highest draw ratios. The $\gamma$ absorption can be divided into two absorptions, i.e. a low-temperature component due to crystal defects and a high-temperature one due to amorphous regions.

**(Keywords: dynamic modulus; poly(oxymethylene); drawing; microwave heating)**

## INTRODUCTION

Poly(oxymethylene) (POM) is one of the most extensively investigated polymers used in the production of ultrahigh-modulus polymers by conventional drawing[1,2], hydrostatic extrusion[3] and die drawing[4]. The physical properties of highly oriented POM have been studied by several investigators[5-9]. Results are summarized in *Table 1*. According to these reports, the attainable draw ratio ($\lambda$) was less than 20 and the highest axial tensile modulus was less than 40 GPa at room temperature.

Recently, it has been shown that ultrahigh-modulus POM with tensile modulus of ~60 GPa (draw ratio > 30) can be produced by tensile drawing under microwave heating[10-12]. Some properties of highly-oriented POM have been reported[13-15]. The crystal modulus of POM has been estimated from the relation between the tensile moduli of highly-oriented tapes and thermal shrinkage caused by annealing[13]. The properties of highly oriented tubes have been assessed by mechanical testing, optical microscopy, scanning electron microscopy, X-ray analysis, birefringence and differential scanning calorimetry[14]. The orientation behaviour of highly oriented tapes has been investigated for $\lambda = 10$–29 (ref. 15).

The investigation of dynamic mechanical behaviour is useful in understanding the molecular mechanisms in highly oriented polymers because several kinds of mechanical absorption are associated with various kinds of molecular chain motion. Previously, dynamic mechanical measurements on uniaxially drawn POM tubes ($\lambda = 1$–33) have been undertaken at only one frequency (3.5 Hz) over the range from −150°C to the melting point; the dynamic moduli and tan $\delta$ have been reported[14]. In the present work, the dynamic mechanical measurements have been extended to several frequencies and data on highly oriented POM tubes with $\lambda \leqslant 41$ have been added. The behaviour of the $\alpha$ and $\gamma$ absorptions is investigated in detail.

0032-3861/86/071030-07$03.00


## EXPERIMENTAL

### *Preparation of samples*

The polymer used was a commercial grade of POM homopolymer, Tenac 3010 (Asahi Chemical Industry Co., Japan), with the following properties: number-average molecular weight, 63 000; melt index, 2.5 g $(10\,\text{min})^{-1}$); density, 1.42 g $\text{cm}^{-3}$; melting point, 175°C (2.5 K $\text{min}^{-1}$); linear expansivity, $8.1 \times 10^{-5}\,\text{K}^{-1}$. Tubes (3 mm o.d., and 1 mm i.d.) were prepared from pellets by extrusion, and highly oriented samples for dynamic mechanical measurements were produced by drawing the tubes under microwave heating[10-12] to draw ratios in the range 11–41. The cross-sectional areas of the samples were determined by weighing a sample of 100 mm length in a microbalance and using an average density of 1.42 g $\text{cm}^{-3}$ (drawn densities varied in the range of 1.41–1.43 g $\text{cm}^{-3}$, regardless of draw ratio[14]). An isotropic sample of 0.5 mm thickness and 6.4 mm width was cut from a compression moulded sheet of the precursor tube. Draw ratios and cross-sectional areas of these samples are summarized in *Table 2*, which also gives ratios of take-up speed and feed speed that show good agreement.

### *Dynamic mechanical measurements*

The dynamic mechanical measurements were performed at four frequencies (3.5, 11, 35 and 110 Hz) on samples 70 mm long using a Rheovibron DDV-3-EA (Toyo Baldwin Co., Japan). The sample length was automatically controlled over the measured temperature range to maintain a constant minimum load of 1 kg. The amplitude of the oscillation was set at $\pm 25\,\mu$m. These conditions correspond to the measurements under strains of about 0.1% for all the samples. Measurements were made between −150°C and the melting point of the sample; the heating rate 1 K $\text{min}^{-1}$. During the heating process, the frequency was changed in the sequence

**Table 1** Summary of prior mechanical investigations[3,5-9]

| Type of specimen | Max. draw ratio | Type of measurement | Frequency (Hz) | Temperature range (°C) | Reference |
|---|---|---|---|---|---|
| Hydrostatically extruded rod | 10 | Axial tensile and shear moduli | — | −196 to 160 | 3 |
| Uniaxially drawn sheet | 19.5 | Dynamic mechanical measurements | 5 | −150 to 20 | 5 |
| | 15 | Axial tensile and shear moduli | — | −150 to 150 | 6 |
| | 16 | Five independent elastic moduli | $10^7$ | −60 to 120 | 6,9 |

**Table 2** Draw ratios and cross-sectional areas of oriented POM

| Speed ratio | 1 | 11 | 15 | 20 | 30 | 40 |
|---|---|---|---|---|---|---|
| Draw ratio | 1 | 11 | 15 | 20 | 28 | 41 |
| Cross-sectional area ($mm^2$) | 3.20 | 0.575 | 0.431 | 0.292 | 0.231 | 0.146 |

110 Hz→35 Hz→11 Hz→3.5 Hz→110 Hz, etc. at intervals of 1 min. The temperature rise per cycle for each frequency was 4 K.

## RESULTS AND DISCUSSION

The magnitude of the complex dynamic tensile modulus ($|E^*|$) was calculated from:

$$|E^*| = \frac{L_0 + \Delta L}{S}\frac{dF}{dL} = \frac{(L_0 + \Delta L)^2}{V}\frac{dF}{dL} \quad (1)$$

where $L_0$ is the initial sample length (70 mm), $\Delta L$ is the displacement in order to maintain the constant minimum load of 1 kg, $S$ and $V$ are the cross-sectional area and the volume of the measured sample, respectively, and $dF$ and $dL$ are the dynamic load and dynamic displacement ($\pm 25$ μm), respectively.

Values for $|E^*|$, $E'$, $E''$, $\tan\delta$ and also $\Delta L$ were automatically printed out.

$$|E^*| = E' + iE''$$
$$E' = |E^*|\cos\delta$$
$$E'' = |E^*|\sin\delta$$

where $E'$ is the storage modulus, $E''$ is the loss modulus and $\delta$ is the phase angle between the viscoelastic stress–strain response. It has been customary to report dynamic mechanical data in terms of the temperature dependence of $E'$ and $\tan\delta$. It was, however, shown by Seferis *et al.*[16] that $E'$ and $E''$ are more sensitive than is $\tan\delta$ to the features of the microstructure. Accordingly, attention will be directed to these quantities.

*Sample length displacement*

The sample length displacements ($\Delta L$) for all the measured samples during the dynamic mechanical measurements are shown in *Figure 1*.

In the undrawn sample ($\lambda = 1$) the sample length increased uniformly with temperature due to high thermal expansivity. In drawn samples with low draw ratios ($\lambda = 11$, 15) the sample length began to decrease with temperatures above 100°C because the shrinkage force overcame the minimum load of 1 kg, and then rapidly increased near the melting point. For highly drawn samples ($\lambda = 20$, 28, 41) the displacement was very small over the measured temperature range. This is due to the decrease of the shrinkage force, i.e. the shrinkage[13] and the sample cross-sectional area decrease with increases in the draw ratio. It is known that the linear expansivity along the draw direction for highly oriented POM is very small[8]. We have also reported that the linear expansivities for highly oriented POM are small negative values of about $-4 \times 10^{-6}\ K^{-1}$ (ref. 17). In all the samples, the sample length displacements were less than 0.7% up to near the melting point.

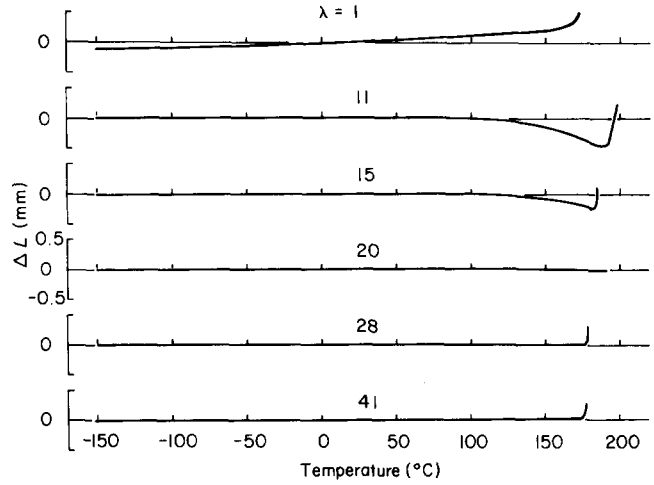


**Figure 1** Sample length displacements during dynamic mechanical measurements

*Dynamic mechanical behaviour*

As examples, values of $E'$ and $E''$ for the undrawn sample and drawn samples are plotted as a function of temperature in *Figures 2, 3* and *4*. The $\alpha$ and $\gamma$ absorptions are clearly discernible even at the higher draw ratios. However, the $\beta$ absorption cannot be observed, even for the undrawn sample. These absorptions are well known[18]. The $\alpha$ absorption is attributed to molecular chain motions in the crystalline regions, and the $\beta$ absorption is due to main-chain micro Brownian motions in the amorphous regions. The $\gamma$ absorption results from local motions of molecular chains in the amorphous regions and at defects within the crystals, but these absorptions are not well understood for highly oriented POM.

It can be seen from *Figures 2* and *3* that the $\alpha$ and $\gamma$ absorptions are drastically enhanced by drawing the isotropic sample only up to the natural draw ratio of about 10. This enhancement corresponds to the increase of $E'$. The $\alpha$ and $\gamma$ absorption peaks reach higher temperatures at the higher frequency. The magnitude of the $\gamma$ absorption is also larger at the higher frequency in

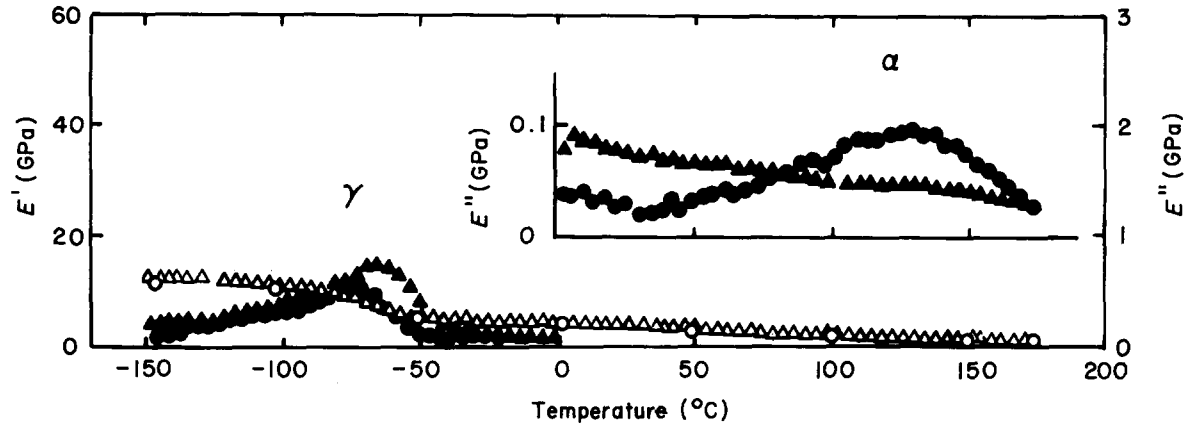


**Figure 2** $E'$: storage modulus (△, ○) and $E''$: loss modulus (▲, ●) for 3.5 Hz (○, ●) and 110 Hz (△, ▲); $\lambda = 1$

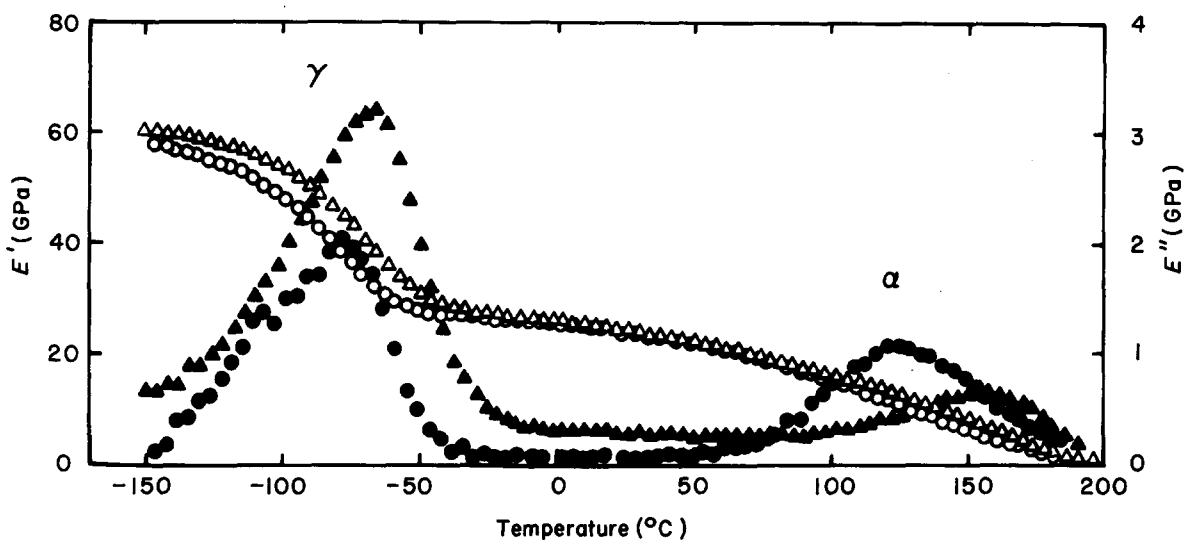


**Figure 3** $E'$: storage modulus (△, ○) and $E''$: loss modulus (▲, ●) for 3.5 Hz (○, ●) and 110 Hz (△, ▲); $\lambda = 11$

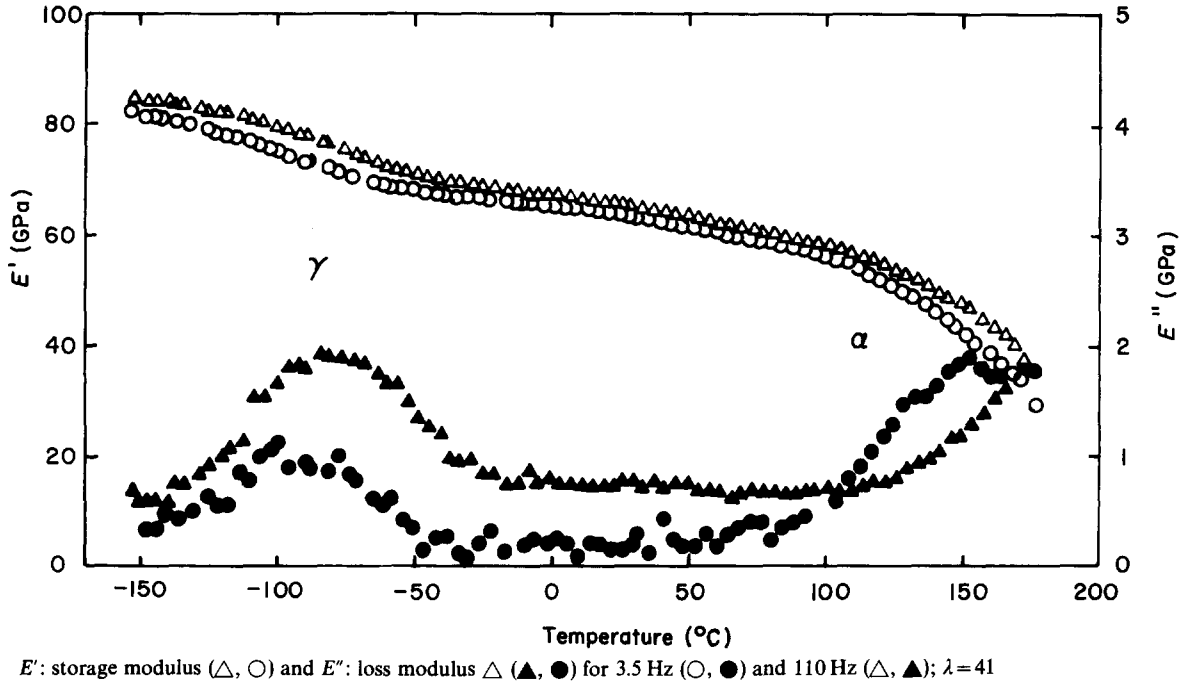


**Figure 4** $E'$: storage modulus (△, ○) and $E''$: loss modulus △ (▲, ●) for 3.5 Hz (○, ●) and 110 Hz (△, ▲); $\lambda = 41$

the measured frequency range, while the magnitude of the α absorption is smaller at the higher frequency.

The γ peak shifts to lower temperatures at the lower draw ratio and the absorption shape becomes more symmetrical for highly oriented samples, as can be seen from *Figures 3* and *4*. The magnitude of the γ absorption decreases for draw ratios above 10 (the natural draw ratio). The α peak shifts to higher temperatures and the magnitude increases with increases in the draw ratio. In all the measured samples the γ absorption occurs in the

temperature range of −150°C to −30°C. The α absorption occurs above 50°C. Since the value of $E'$ is almost zero at the melting point, the value of $E'$ at room temperature reflects the magnitude of the α absorption, while the value of $E'$ at −150°C reflects the magnitudes of both absorptions (α and γ).

The draw ratio dependence of $E'$ (3.5 Hz) at −150, 20 and 150°C is shown in *Figure 5*. These $E'$ values increase with increases in the draw ratio. The increase of $E'$ at −150°C is especially remarkable near $\lambda = 10$. For the most highly oriented sample ($\lambda = 41$), the highest $E'$ values at 3.5 Hz were 82, 64 and 42 GPa at −150, 20 and 150°C, respectively.

The maximum $E'$ of 85 GPa was obtained at 110 Hz and −150°C for the most highly oriented sample ($\lambda = 41$), as shown in *Figure 4*. In the calculation of $|E^*|$ (equation (1)), the temperature dependence of $S$ (or $V$) was not taken into account. The cross-sectional area, determined at room temperature from the weight of a length of sample with a constant density of 1.42 g cm$^{-3}$, was used for $S$ over the measured temperature range. Although the thermal expansivity of oriented POM along the draw direction is very small, the expansivity normal to the draw direction is large even for highly oriented POM[8]. The average linear expansivity is about $1 \times 10^{-4}$ K$^{-1}$. Therefore, the values for $|E^*|$ are underestimated at lower temperatures and overestimated at higher temperatures. For example, the correction reaches about 5% at −150°C. Then the corrected maximum $E'$ becomes 89 GPa at 110 Hz and −150°C. This value exceeds any reported experimental values for highly-oriented POM samples[1-9].

*γ Absorption*

The Arrhenius plots for the γ absorption peak are shown in *Figure 6*. For comparison, the data on dielectric absorption[19] are also plotted in the figure. Dielectric measurements were made for POM prepared from tetra(oxymethylene) crystals by solid-state polymerization. The samples were uniaxially oriented POM crystals in which amorphous regions, except for crystal defects, do not exist.

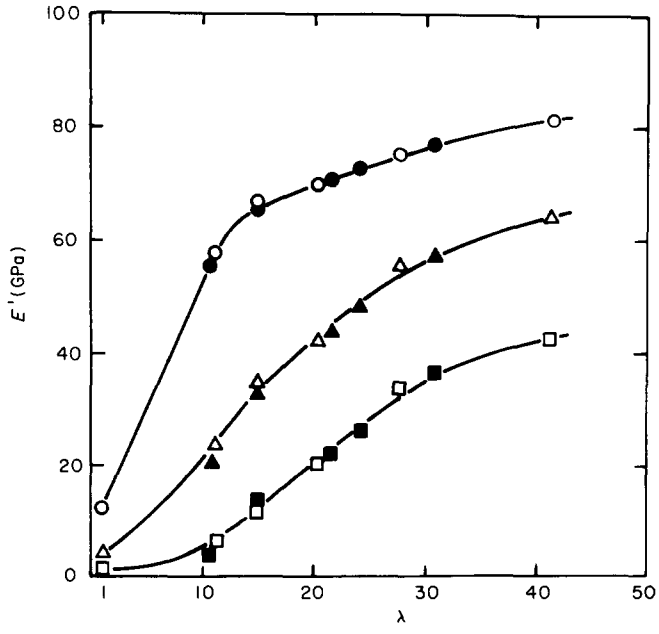


**Figure 5** Dependence of storage modulus ($E'$) at 3.5 Hz on draw ratio ($\lambda$) for this study (○, △, □) and for previous research[14] (●, ▲, ■); (○, ●) −150°C; (△, ▲) 20°C; (□, ■) 150°C

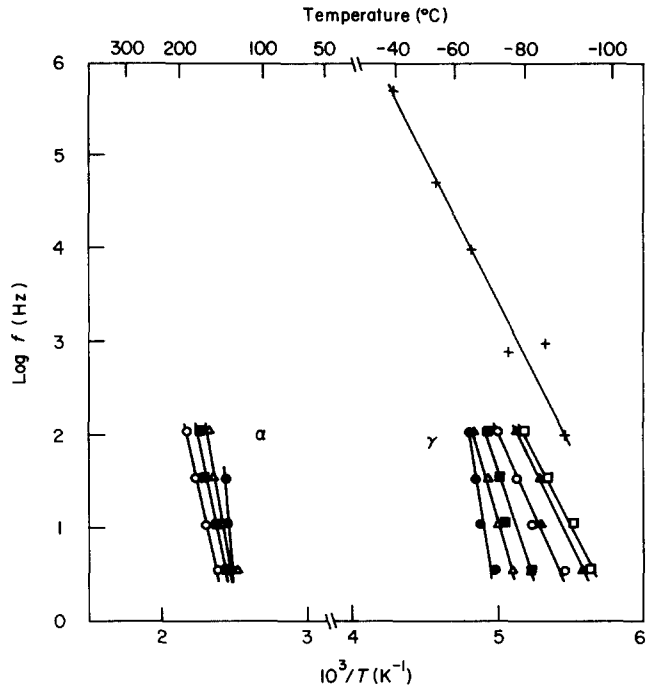


**Figure 6** log $f$ *versus* $T^{-1}$ for the loss modulus maxima of the α and γ absorptions. Draw ratios: (●) 1, (△) 11, (■) 15, (○) 20, (▲) 28, (□) 41. Also shown are dielectric data (+) on POM crystals[19]

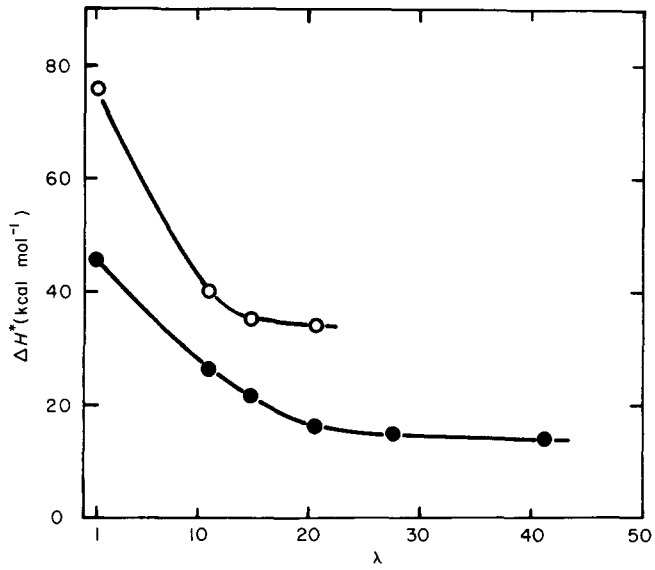


**Figure 7** Activation energy *versus* draw ratio: (○) α absorption; (●) γ absorption

Linear relations were observed for all the samples in the measured frequency range. The γ peak moves to lower temperatures with increases in the draw ratio. For example, the peak temperature at 3.5 Hz shifts from −72°C ($\lambda = 1$) to −95°C ($\lambda = 41$). The γ peak temperature for POM crystals is extrapolated from the dielectric data to be −104°C at 3.5 Hz. This temperature is considered to be an ultimate temperature for the γ peak temperature of highly drawn POM samples.

The activation energy ($\Delta H^*$) was evaluated from the slope of the plot log $f$ versus $T^{-1}$ (*Figure 6*) which has a slope $\Delta H^*(2.303R)^{-1}$, where $R$ is the gas constant. The draw ratio dependence of $\Delta H^*$ is shown in *Figure 7*. $\Delta H^*$ for the undrawn sample was 46 kcal mol$^{-1}$. $\Delta H^*$

decreases with increases in the draw ratio and then becomes a constant value, of about 14 kcal $mol^{-1}$ when $\lambda > 20$. This value coincides with that obtained for POM crystals from the dielectric measurements (*Figure 6*). This means that the $\gamma$ absorption for highly drawn samples is like that for uniaxially oriented POM crystals with crystal defects, although the $\gamma$ peak temperature is still about 10 K higher than that for the POM crystals.

The decrements in $E'$ ($\Delta E'$) were obtained in order to evaluate the magnitude of the $\gamma$ absorption. The $\gamma$ absorption occurs in the temperature range between $-150$°C and $-30$°C, as shown in *Figures 2, 3* and *4*. The value of $\Delta E'$ is the difference of the $E'$ values at $-150$°C and $-30$°C. The draw ratio dependence of $\Delta E'$ is shown in *Figure 8*. The rapid increase of $\Delta E'$ up to $\lambda = 10$ seems to be due to the molecular orientation because the crystalline orientation function almost reaches unity up to $\lambda = 10$ (refs. 9 and 15). Increases in $E'$ and $E''$ along the draw direction due to molecular orientation have also been observed for drawn polypropylene films[16]. The decrease of $\Delta E'$ above $\lambda = 10$ seems to be mainly due to a decrease in the amorphous fraction.

The $\gamma$ absorption for the undrawn sample is asymmetrical (as shown in *Figure 2*). This asymmetry has been ascribed to the superposition of two absorptions, i.e. a low-temperature component ($\gamma_c$) due to crystal defects and a high-temperature one ($\gamma_a$) due to amorphous regions[19]. An attempt was made to divide the $\gamma$ absorption for drawn POM into the two components, $\gamma_c$ and $\gamma_a$. The first trial was made for the $\gamma$ absorption data at 110 Hz because the magnitude is larger than that at 3.5 Hz. The results are shown in *Figure 9*. In $E''$–temperature plots the background values of $E''$ were subtracted in order to minimize the influence of all

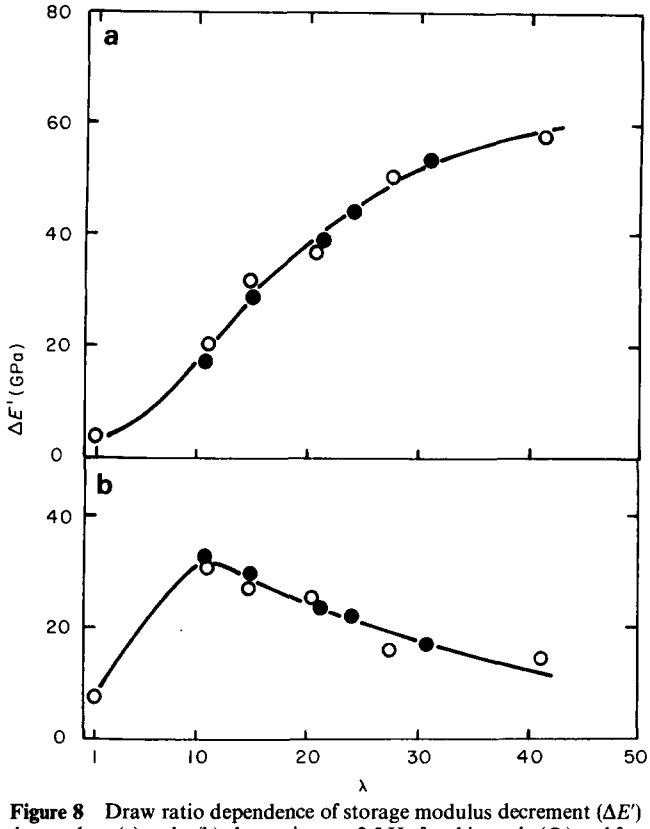


**Figure 8** Draw ratio dependence of storage modulus decrement ($\Delta E'$) due to the $\alpha$ (a) and $\gamma$ (b) absorptions at 3.5 Hz for this study (○) and for previous research[14] (●)

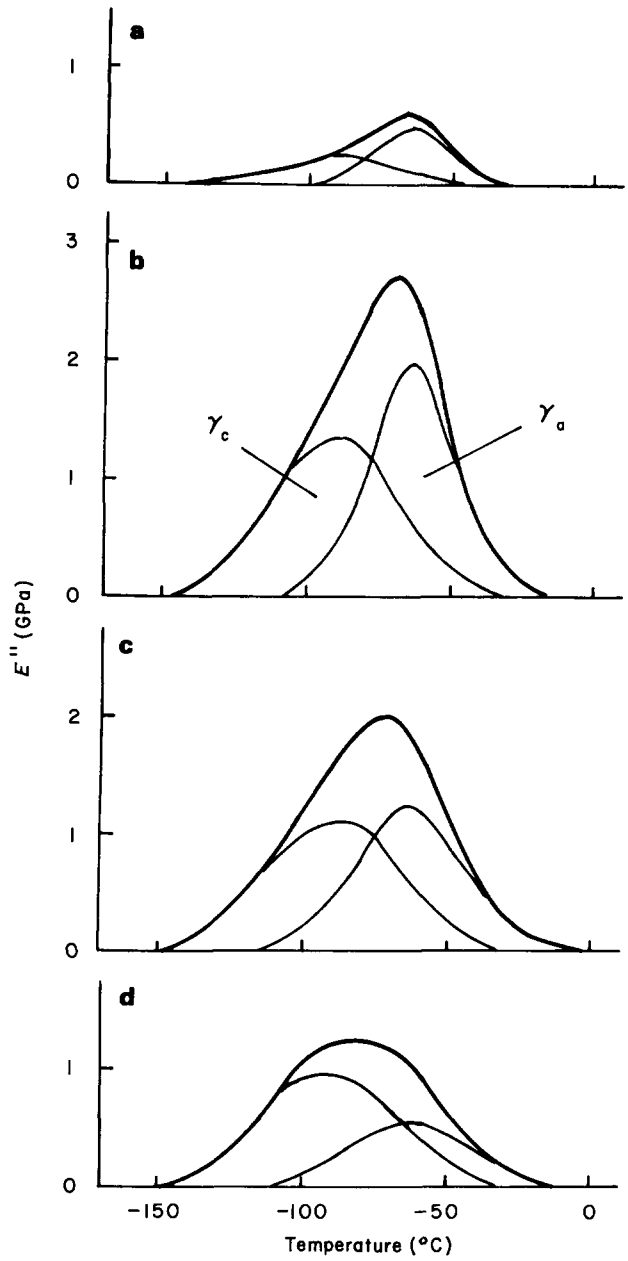


**Figure 9** Decomposition (at 110 Hz) of the $\gamma$ absorption into $\gamma_c$ and $\gamma_a$ components. Draw ratios: (a) 1, (b) 11, (c) 20, (d) 41

absorptions other than the $\gamma$ absorption. It was assumed that the location of the $\gamma_c$ absorption in the drawn POM is same as that of the $\gamma$ absorption observed for POM crystals in the dielectric measurements[19]. An exception was expected for the magnitude, i.e. the peak temperature is located at $-90$°C and the shape is symmetrical. It was also assumed that the shape of the $\gamma_a$ absorption is symmetrical.

First, the low temperature side of the $\gamma$ absorption was reflected to the high temperature side with respect to a vertical axis at $-90$°C. Then, the difference between the original $E''$ values and the reflected ones was plotted. In this way, the $\gamma_a$ absorption with a peak temperature of $-63$°C was drawn, although the low temperature side of the $\gamma_a$ absorption was not yet clear. Next, the high temperature side of the $\gamma_a$ absorption was reflected to the low temperature side with respect to a vertical axis at $-63$°C. By plotting the difference between the original $E''$ values and the reflected ones, the $\gamma_c$ absorption was drawn.

As shown in *Figure 9*, the absorption can be divided into two symmetrical ($\gamma_c$ and $\gamma_a$) absorptions for which the peak temperatures are located at −90°C and −63°C, respectively, regardless of the draw ratio.

The draw ratio dependence of the $\gamma$ peak temperature at 110 Hz is shown in *Figure 10*. For the undrawn sample, the peak temperature (−65°C) is almost equal to the $\gamma_a$ peak temperature (−63°C). The $\gamma$ peak temperature approaches the $\gamma_c$ peak temperature (−90°C) as the draw ratio increases. The draw ratio dependences of $E''_{max}$ for the $\gamma$, $\gamma_c$ and $\gamma_a$ absorptions at 110 Hz are shown in *Figure 11*. All these $E''_{max}$ values increase up to $\lambda = 10$ and then decrease with increases in the draw ratio. The $E''_{max}$ for the $\gamma_a$ absorption is more sensitive to changes in the draw ratio than that for the $\gamma_c$ absorption.

It was difficult to determine the crystallinity ($X_c$) for highly oriented POM from the density because the density was affected by voids[14]. Thus, $X_c$ was determined from pulsed n.m.r. measurements for highly oriented POM tapes[15]. Applying the relationship between crystallinity and draw ratio, the $X_c$ values for the measured samples were estimated. The relationship between $E''_{max}$ and the amorphous fraction ($X_a = 1 - X_c$) for the $\gamma_c$ and $\gamma_a$ absorptions are shown in *Figure 12*. The $E''_{max}$ for the $\gamma_a$ absorption is closely correlated with $X_a$, i.e. the value becomes zero at $X_a = 0$ and increases linearly with

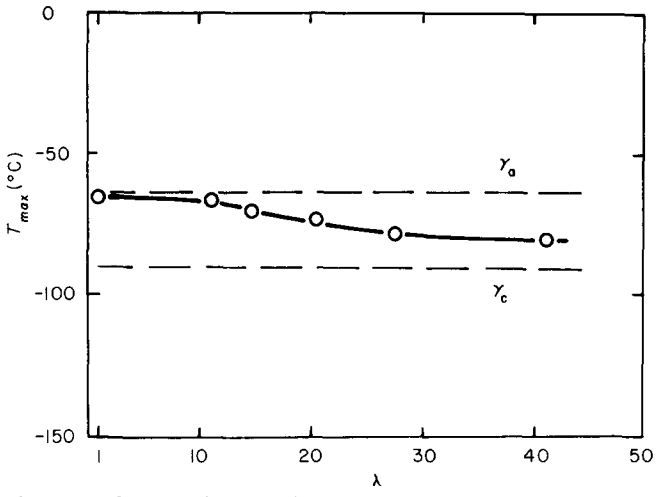


**Figure 10** Draw ratio dependence of $E''_{max}$ temperature for the $\gamma$ absorption at 110 Hz

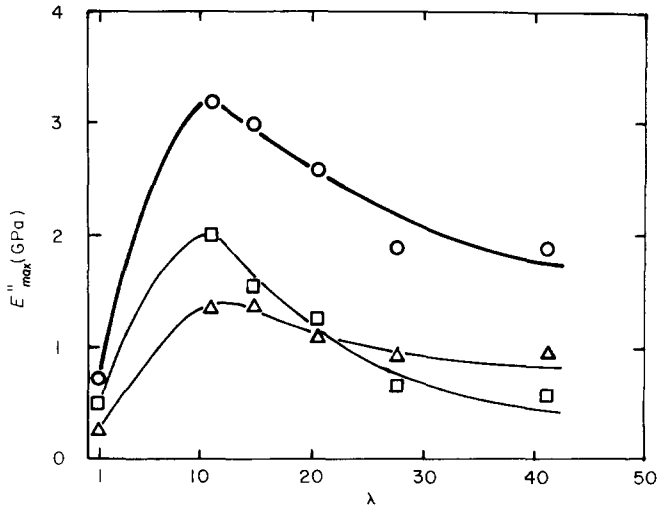


**Figure 11** Draw ratio dependence of $E''_{max}$ for the $\gamma$ absorption at 110 Hz: (○) $\gamma$ absorption; (△) $\gamma_c$ absorption; (□) $\gamma_a$ absorption

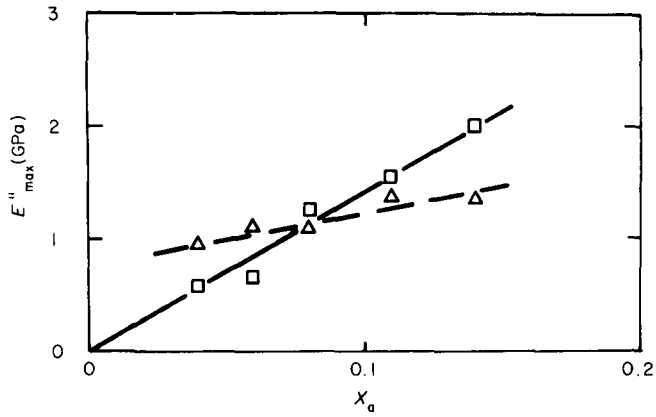


**Figure 12** $E''_{max}$ *versus* amorphous fraction ($X_a$): (△), $\gamma_c$ absorption; (□), $\gamma_a$ absorption

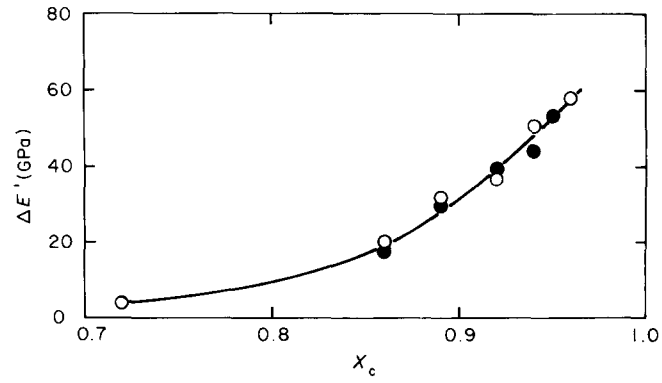


**Figure 13** Crystallinity ($X_c$) dependence of storage modulus decrement ($\Delta E'$) due to α absorption at 3.5 Hz for (○) this study and for (●) previous research[14]

$X_a$. This means that the $\gamma_a$ absorption can be attributed to local motions in the amorphous regions. On the other hand, the $E''_{max}$ value for the $\gamma_c$ absorption at $X_a = 0$ (extrapolated from the line in *Figure 12*) does not become zero, even though the measured values produce a decreasing function for $X_a$. This means that crystal defects will probably exist even when $X_a = 0$ ($X_c = 1$). Consequently, the $\gamma$ absorption for highly drawn POM can be decomposed into the $\gamma_c$ and $\gamma_a$ absorptions by this method. The shift of the $\gamma$ absorption peak to lower temperatures with increase in the draw ratio and the symmetry at the higher draw ratios can be explained in terms of decrease in the magnitude of the $\gamma_a$ absorption.

*α Absorption*

The Arrhenius plots for the α absorption peak are shown in *Figure 6*. For the most highly oriented samples in this study ($\lambda = 28, 41$), the peaks move to points above the melting points at the higher frequencies of 35 and 110 Hz. Therefore, such data were not obtained. The α peak moves to higher temperatures with increases in the draw ratio. For example, the α peak temperature at 3.5 Hz shifts from 128°C ($\lambda = 1$) to 150°C ($\lambda = 41$). The draw ratio dependence of the activation energy ($\Delta H^*$) is shown in *Figure 7*. $\Delta H^*$ decreases rapidly from 76 kcal mol$^{-1}$ for the undrawn sample to less than 40 kcal mol$^{-1}$ at $\lambda \sim 10$, at which the crystalline orientation function almost reaches unity[15].

The α absorption occurs in the temperature range between 50°C and the melting point. The decrement in $E'$ ($\Delta E'$) due to the α absorption is thus considered to be the difference between the $E'$ values taken at 50°C and the

melting point. At the melting point the value of $E'$ is almost zero. Thus, the $\Delta E'$ is the value of $E'$ at 50°C. The draw ratio dependence of $\Delta E'$ for the $\alpha$ absorption is shown in *Figure 8*. $\Delta E'$ continues to increase with increases in draw ratio. The relation between $\Delta E'$ and $X_c$, determined from pulsed n.m.r. measurements for highly oriented POM tapes[15], is shown in *Figure 13*. The increase of $\Delta E'$ for the $\alpha$ absorption is closely correlated with the increase of crystallinity. The dynamic modulus $E'$ at room temperature mainly reflects the magnitude of the $\alpha$ absorption. The draw ratio dependence of the dynamic modulus at room temperature has been already explained in terms of crystallinity and taut-tie molecular fraction for highly oriented POM tapes[15].

## CONCLUSIONS

Ultrahigh-modulus POM can be produced by microwave heat-drawing. The dynamic modulus at 110 Hz reaches a value of 85 GPa at $-150$°C for the most highly oriented sample studied ($\lambda = 41$). The modulus exceeds 40 GPa even at 150°C.

The $\alpha$ and $\gamma$ absorptions are clearly discernible even at the highest draw ratios. The $\gamma$ absorption peak falls with increase in draw ratio. The activation energy decreases from 46 kcal mol$^{-1}$ for the undrawn sample to a constant value of bout 14 kcal mol$^{-1}$ for $\lambda > 20$; the latter value coincides with that for uniaxially oriented POM crystals with no amorphous regions. The magnitude of the $\gamma$ absorption increases to a maximum ($\lambda \sim 10$) and then decreases. The initial increase is attributed to the molecular orientation in the amorphous regions and crystal defects. The $\gamma$ absorption can be divided into two components, i.e. a low-temperature one, $\gamma_c$, which is due to crystal defects, and a high-temperature one, $\gamma_a$, which is due to amorphous regions.

The $\alpha$ absorption peak shifts to higher temperatures with increase in draw ratio. The activation energy decreases rapidly from 76 kcal mol$^{-1}$ for the undrawn sample to less than 40 kcal mol$^{-1}$ at $\lambda \sim 10$, at which the crystalline regions orient almost perfectly in the draw direction. The magnitude of the $\alpha$ absorption increases with increase in the draw ratio, reflecting an increase in crystallinity.

## REFERENCES


1 Clark, E. S. and Scott, L. S. *Polym. Eng. Sci.* 1974, **14**, 682
2 Brew, B. and Ward, I. M. *Polymer* 1978, **19**, 1338
3 Coates, P. D. and Ward, I. M. *J. Polym. Sci., Polym. Phys. Edn.* 1978, **16**, 2031
4 Hope, P. S., Richardson, A. and Ward, I. M. *J. Appl. Polym. Sci.* 1981, **26**, 2879
5 Brew, B., Clements, J., Davies, G. R., Jakeways, R. and Ward, I. M. *J. Polym. Sci., Polym. Phys. Edn.* 1979, **17**, 351
6 Leung, W. P., Chan, C. C., Chen, F. C. and Choy, C. L. *Polymer* 1980, **21**, 1148
7 Choy, C. L., Chen, F. C. and Luk, W. H. *J. Polym. Sci., Polym. Phys. Edn.* 1980, **18**, 1187
8 Choy, C. L., Chen, F. C. and Young, K. *J. Polym. Sci., Polym. Phys. Edn.* 1981, **19**, 335
9 Choy, C. L., Leung, W. P. and Huang, C. W. *Polym. Eng. Sci.* 1983, **23**, 910
10 Nakagawa, K., Maeda, O. and Yamakawa, S. *J. Polym. Sci., Polym. Lett. Edn.* 1983, **21**, 933
11 Nakagawa, K., Konaka, T. and Yamakawa, S. *Polymer* 1985, **26**, 84
12 Nakagawa, K. and Konaka, T. *Polymer* 1986, **27**, 1037–1043
13 Takeuchi, Y., Yamamoto, F. and Nakagawa, K. *J. Polym. Sci., Polym. Lett. Edn.* 1984, **22**, 159
14 Konaka, T., Nakagawa, K. and Yamakawa, S. *Polymer* 1985, **26**, 462
15 Takeuchi, Y., Yamamoto, F., Nakagawa, K. and Yamakawa, S. *J. Polym. Sci., Polym. Phys. Edn.* 1985, **23**, 1193
16 Seferis, J. C., McCullough, R. L. and Samuels, R. *J. Appl. Polym. Symp.* 1975, No. 27, 205
17 Yamamoto, F., Nakagawa, K., Shuto, Y. and Yamakawa, S. *Electron. Lett.* 1983, **19**, 674
18 McCrum, N. G., Read, B. E. and Williams, G. 'Anelastic and Dielectric Effects in Polymeric Solids', John Wiley and Sons, London, 1967, p. 540
19 Tanaka, A., Uemura, S. and Ishida, Y. *J. Polym. Sci. A-2* 1970, **8**, 1585